A small molecule redistributes iron in ferroportin-deficient mice and patient-derived primary macrophages

Stella Ekaputri[a], Eun-Kyung Choi[b], Manuela Sabelli[c] ⓘ, Luisa Aring[b] ⓘ, Kelsie J. Green[d], JuOae Chang[e], Kai Bao[f], Hak Soo Choi[f] ⓘ, Shigeki Iwase[g], Jonghan Kim[e,h] ⓘ, Elena Corradini[c], Antonello Pietrangelo[c,1] ⓘ, Martin D. Burke[d,i,j,k,1], and Young Ah Seo[b,1] ⓘ

Deficiencies of the transmembrane iron-transporting protein ferroportin (FPN1) cause the iron misdistribution that underlies ferroportin disease, anemia of inflammation, and several other human diseases and conditions. A small molecule natural product, hinokitiol, was recently shown to serve as a surrogate transmembrane iron transporter that can restore hemoglobinization in zebrafish deficient in other iron transporting proteins and can increase gut iron absorption in FPN1-deficient flatiron mice. However, whether hinokitiol can restore normal iron physiology in FPN1-deficient animals or primary cells from patients and the mechanisms underlying such targeted activities remain unknown. Here, we show that hinokitiol redistributes iron from the liver to red blood cells in flatiron mice, thereby increasing hemoglobin and hematocrit. Mechanistic studies confirm that hinokitiol functions as a surrogate transmembrane iron transporter to release iron trapped within liver macrophages, that hinokitiol-Fe complexes transfer iron to transferrin, and that the resulting transferrin-Fe complexes drive red blood cell maturation in a transferrin-receptor–dependent manner. We also show in FPN1-deficient primary macrophages derived from patients with ferroportin disease that hinokitiol moves labile iron from inside to outside cells and decreases intracellular ferritin levels. The mobilization of nonlabile iron is accompanied by reductions in intracellular ferritin, consistent with the activation of regulated ferritin proteolysis. These findings collectively provide foundational support for the translation of small molecule iron transporters into therapies for human diseases caused by iron misdistribution.

hinokitiol | iron misdistribution | ferroportin disease | iron redistribution | hemoglobinization

FPN1 is a 12-transmembrane helix protein present in the plasma membrane and is the only known cellular iron exporter identified in mammals (1–3). It plays a key role in iron recycling by releasing iron from the reticuloendothelial system including liver and spleen macrophages following erythrophagocytosis. FPN1 is regulated posttranslationally by hepcidin, a peptide hormone that induces the internalization and degradation of FPN1 (4). Loss of FPN1 function due to genetic deficiency or dysregulation of hepcidin thus causes systemic iron misdistribution marked by iron accumulation in the liver and iron deficiency in bone marrow leading to anemia (5, 6) (Fig. 1A). This pathophysiology is commonly found in a range of human diseases that are driven by FPN1 dysfunction (7–10). Loss-of-function mutations in the *FPN1* gene cause ferroportin disease (FD) (11), which is characterized by mild anemia with liver iron overload (12). Induced FPN1 deficiencies caused by hepcidin dysregulation underlie the genetic disease iron refractory iron deficiency anemia (13) as well as anemia of inflammation, a condition found in millions of patients worldwide, including those with chronic kidney disease (14), rheumatoid arthritis (15), lupus (16), inflammatory bowel disease (17), diabetes (18), cardiovascular disease (19), cystic fibrosis (20), cancer (21), and aging (22). As with many human diseases caused by loss of protein function, these conditions are still treated primarily with suboptimal therapies that fail to address the underlying functional defect, including regular venesection (23) and/or iron chelators (24, 25). In the present study, we envisioned an alternative approach in which a small molecule surrogate for FPN1 would redistribute iron from liver macrophages to bone marrow to reestablish iron homeostasis (Fig. 1A). We specifically hypothesized that this could be achieved via a three-step mechanism involving 1) small-molecule-mediated release of iron from where it is trapped within FPN1-deficient macrophages in the liver, 2) transfer of iron atoms from the small molecule to transferrin (Tf), and 3) holo-Tf-mediated hemoglobinization (Fig. 1B).

Previously, we reported that a small molecule natural product, hinokitiol, can perform protein transporter-like iron mobilization in a site- and direction-selective manner by harnessing the transmembrane iron gradients that build up where protein iron transporters are missing (26). We demonstrated that hinokitiol increases gut iron absorption

Significance

Iron misdistribution underlies various diseases, ranging from anemia to neurodegeneration, but approaches to addressing this general problem are lacking. We recently reported that a small molecule natural product, hinokitiol, is capable of restoring hemoglobinization in various animal models with missing iron transporters. We now show that hinokitiol is capable of redistributing iron systemically, which in turn restores iron homeostasis in ferroportin-deficient mice and in primary macrophages derived from patients with ferroportin disease. We also elucidated the stepwise mechanism of hinokitiol-mediated iron redistribution and physiological restoration. Together, these results provide foundational support for using a molecular prosthetics approach for better understanding and possibly treating iron misdistribution.
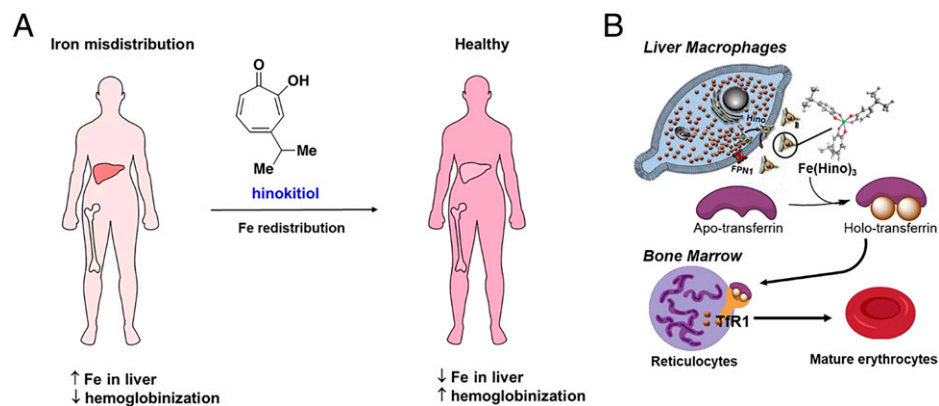
Fig. 1. Hypothesis for hinokitiol-mediated iron redistribution and hemoglobinization. (*A*) A small molecule is hypothesized to redistribute iron from the liver to RBCs and restore hemoglobinization. (*B*) Potential stepwise mechanism for hinokitiol-mediated hemoglobinization via a transferrin-dependent pathway.

in divalent metal transporter 1 (DMT1)-deficient Belgrade rats and FPN1-deficient flatiron (*ffe*/+) mice, as well as induces hemoglobinization in mitoferrin (MFRN1)-deficient zebrafish. However, whether hinokitiol can redistribute iron and thereby restore normal iron physiology in FPN1-deficient animals or primary cells from patients, and the mechanisms underlying such targeted activities, remain unresolved.

In the present study, we demonstrate that hinokitiol can redistribute iron from the liver to red blood cells (RBCs) in FPN1-deficient *ffe*/+ mice, thereby promoting hemoglobinization. We also characterize the mechanism of this process, including a key step in which iron atoms are readily transferred from hinokitiol to Tf, thereby permitting RBC maturation via a Tf-dependent pathway. Finally, we demonstrate that hinokitiol can mobilize iron and promote ferritin degradation in primary macrophages obtained from patients with FD. Collectively, these studies provide strong foundational support for the use of small molecule iron mobilizers to better understand iron misdistribution and possibly to better treat human diseases caused by the loss of FPN1 function.

Results

Hinokitiol Restores Hemoglobinization in Flatiron Mice by Redistributing Iron from the Liver to RBCs. In this study, we utilized *ffe*/+ mice, which harbor an H32R loss-of-function mutation in FPN1 (27). As the leading animal model of FD, *ffe*/+ mice display some important features similar to the clinical manifestations in humans, such as iron buildup in the liver, reduced levels of Tf saturation, and mild anemia (23, 28, 29). As a point of reference, loss-of-function mutations in FD similarly result in mild anemia in patients (11).

Consistent with previous reports (30), *ffe*/+ mice showed higher nonheme iron levels in the liver (Fig. 2*A*), spleen (*SI Appendix*, Fig. S1*A*), and duodenum (*SI Appendix*, Fig. S1*C*) compared with wildtype controls. Four hours after intraperitoneal (IP) administration of various doses of hinokitiol (acute treatment), we observed a significant reduction of liver nonheme iron of *ffe*/+ mice in a dose-dependent manner (Fig. 2*A*). We also quantified total liver iron and observed a similar and even larger reduction upon treatment with increasing doses of hinokitiol (Fig. 2*B*). These data suggested the potential capacity for hinokitiol to reduce nonlabile iron in the tissue, possibly by mobilizing the labile iron pool. Notably, at the highest dose tested, liver iron levels were reduced to wildtype-like levels, but not lower (Fig. 2 *A* and *B*). On a percentage basis, the splenic nonheme and total iron were not reduced upon hinokitiol

administration (*SI Appendix*, Fig. S1 *A* and *B*). Additionally, nonheme and total iron concentrations in the duodenum were also unchanged by hinokitiol (*SI Appendix*, Fig. S1 *C* and *D*). Furthermore, hinokitiol did not perturb the homeostasis of other metals in the same mice (*SI Appendix*, Fig. S2 *A–I*). These data suggest that hinokitiol primarily promotes the release of iron retained in the livers of flatiron mice.

Next, we investigated the physiological consequences of iron mobilization by chronic administration of hinokitiol at 10 mg/kg daily for 1 wk. This low dose treatment again reduced liver nonheme iron levels (Fig. 2*C*) but showed no statistically significant effect on nonheme iron levels in the spleen and duodenum (*SI Appendix*, Fig. S1 *E* and *F*). Additionally, we observed increased serum iron (Fig. 2*D*) and Tf saturation (Fig. 2*E*) in hinokitiol-treated *ffe*/+ mice, suggesting that iron is released from the liver into the systemic circulation, followed by transfer from the small molecule to Tf (see below). The serum ferritin level was unchanged (*SI Appendix*, Fig. S1*G*), but the increased Tf saturation was sufficiently increased to induce hemoglobinization in *ffe*/+ mice, as indicated by the statistically significant improvement in hematocrit (Fig. 2*F*) and hemoglobin (Fig. 2*G*) levels. Specifically, we observed a statistically significant change ($P < 0.05$) in the hematocrit levels from $49.4 \pm 0.8\%$ in nontreated *ffe*/+ mice to $52.6 \pm 0.8\%$ in the hinokitiol-treated group, which is similar to the wildtype level of $52.4 \pm 0.8\%$ (Fig. 2*F*). Consistently, hemoglobin levels also significantly increased from 16.9 ± 0.2 g/dL in nontreated *ffe*/+ mice to 19 ± 0.3 g/dL ($P < 0.001$) in the hinokitiol-treated group, which is similar to the hemoglobin level of 18.7 ± 0.4 g/dL found in the wildtype mice (Fig. 2*G*).

Notably, the partial recovery of serum iron and Tf saturation was associated with complete recovery of hemoglobin and hematocrit. Prior studies show that mice can regenerate ~15 to 20% of their RBCs/hemoglobin every 7 d (31). Thus, our findings are consistent with the conclusion that erythropoietic cells can use the mobilized iron from macrophages to produce more hemoglobin. It is also notable that hinokitiol treatment restored Tf saturation, hematocrit, and hemoglobin levels to wildtype-like values but not higher. These data suggest that hinokitiol reestablishes homeostasis impaired by FPN1 deficiencies.

Hinokitiol Mobilizes Iron out of FPN1-Deficient Macrophages In Vitro. Having established the hinokitiol-mediated reduction of liver iron levels and restoration of hemoglobinization in vivo (Fig. 2 *A* and *B*), we next aimed to elucidate the mechanistic underpinnings of this process. Although we did not exclude the possibility that hinokitiol mobilized iron from hepatocytes
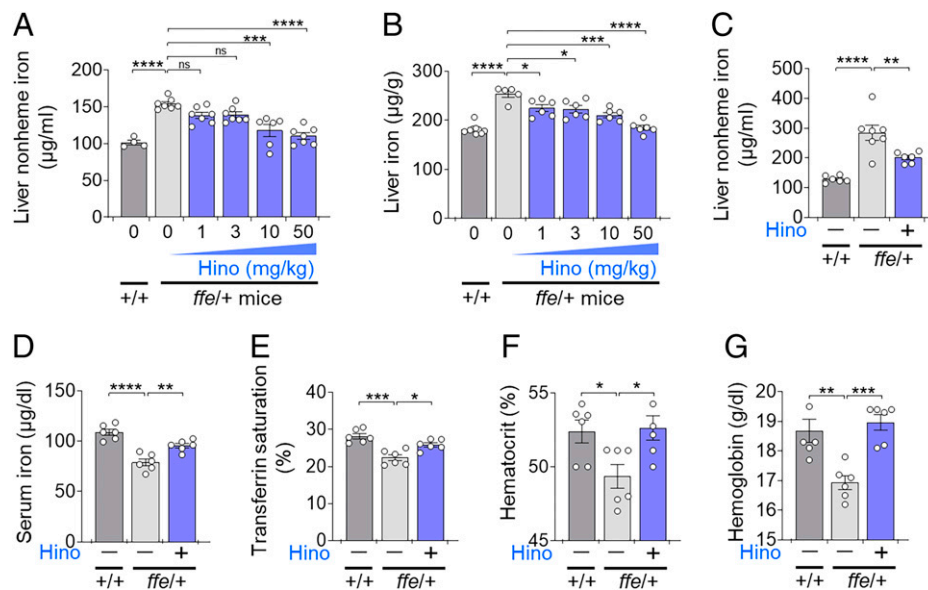
Fig. 2. Hinokitiol restores iron physiology in flatiron mice by mobilizing iron from sites of accumulation. (*A*) Liver nonheme iron and (*B*) total iron measured 4 h after acute hinokitiol (Hino) administration. (*C–G*) Flatiron mice treated for 7 d IP with 10 mg/kg Hino show (*C*) a decrease in liver nonheme iron and increases in (*D*) serum iron and (*E*) transferrin saturation. These changes are accompanied by restored (*F*) hematocrit and (*G*) hemoglobin. (*F*) Hematocrit: 52.4 ± 0.8% for $^{+/+}$, 49.4 ± 0.8% for nontreated *ffe*/+, and 52.6 ± 0.8% for hinokitiol-treated *ffe*/+ mice. Hematocrit increase in *ffe*/+ mice treated with hinokitiol was statistically significant ($P < 0.05$). (*G*) Hemoglobin: 18.7 ± 0.4 g/dL for $^{+/+}$, 16.9 ± 0.2 g/dL for nontreated *ffe*/+, and 19 ± 0.3 g/dL for hinokitiol-treated *ffe*/+ mice. Hemoglobin increase in *ffe*/+ mice treated with hinokitiol was statistically significant ($P < 0.001$). Results are means ± SEM ($n = 5$ to 8 mice/group). Three independent experiments were performed yielding similar results. *$P < 0.05$, **$P < 0.01$, ***$P < 0.001$, and ****$P < 0.0001$ by one-way ANOVA with Tukey's multiple comparison test.

(Fig. 2 *A* and *B*), we hypothesized that the first step in iron redistribution involves iron release from liver macrophages (Kupffer cells). This is due to the fact that the associated liver disease in FD patients is not as severe as in hemochromatosis patients (32). Moreover, anemia associated with FD is due to iron retention in FPN1-deficient macrophages that perturbs effective erythropoiesis (4, 33, 34).

We used a RAW264.7 macrophage cell line that has been widely used for CRISPR-Cas9 gene editing (35, 36) to generate FPN1-knockout (KO) macrophages (Δ*FPN1* cells). We observed complete abrogation of FPN1 protein levels (Fig. 3*A*) due to the corresponding deletions (*SI Appendix,* Fig. S3). We acknowledge that levels of the GAPDH protein, which we used as a control, can be somewhat regulated by iron levels (37), but we saw very little change in the intensity of this band. This cell line also displayed intracellular accumulation of labile iron as detected by the turn-off iron probe calcein (Fig. 3*B*). Following hinokitiol treatment, iron release was assayed using radioactive iron, whereas intracellular labile iron was probed using calcein. Hinokitiol treatment induced a robust ^{55}Fe release (Fig. 3*C*), along with an up to 1.5-fold reduction in intracellular labile iron levels in a concentration-dependent manner (Fig. 3*D*). The highest hinokitiol concentration used in the calcein assay similarly induced ^{55}Fe release (*SI Appendix, Fig. S4 A–C*), indicating that both methods can be used to measure iron mobilization.

We also isolated primary Kupffer cells from *ffe*/+ mice and their wildtype littermates. The purity of the preparations was assessed by specific markers, as follows: *Albumin* for hepatocytes, *Cd45* for Kupffer cells, and *Cd146* for endothelial cells. High levels of *Cd45* were expressed in Kupffer cells isolated from *ffe*/+ mice and their wildtype littermates (Fig. 3*E*). Hinokitiol treatment restored iron transport in *ffe*/+-derived Kupffer cells (Fig. 3*F*) and reduced intracellular iron accumulation (Fig. 3*G*). Collectively, these in vitro data demonstrate that hinokitiol mobilizes intracellularly-accumulated iron from FPN1-deficient macrophages into the extracellular space (Fig. 1*B*).

Transfer of Hinokitiol-Bound Iron to apo-Tf Induces Hemoglobinization. We next probed the second step of our mechanistic hypothesis in which the small molecule hinokitiol transfers its bound iron to apo-Tf (Fig. 1*B*). Three molecules of hinokitiol bind to one iron atom to form an Fe(Hino)$_3$ complex (26). When we mixed increasing equivalents of preformed Fe(Hino)$_3$ complex with apo-Tf, we observed increased levels of iron transferred from the small molecule to the protein (Fig. 4*A*).

Tf contains two similar but nonhomologous binding sites, termed the C-terminal and N-terminal sites. Iron binding to Tf is sequential; iron binds to either the C-terminal or N-terminal site to form monoferric Tf first before holo-Tf formation is possible (38). Accordingly, we calculated the relative iron-binding constants K_{eq} of each Tf terminal site following iron transfer from the Fe(Hino)$_3$ complex (*SI Appendix, Table S2*) (39). Due to the differences in their chemical properties, four Tf species can be separated using urea gel electrophoresis to quantify their molar fractions (Fig. 4*A*). We calculated the percentage of Tf iron saturation resulting from apo-Tf incubation with various concentrations of Fe(Hino)$_3$ according to the equation shown in *SI Appendix,* Appendix S1 (*SI Appendix, Fig. S5A*). The average ratios of the site binding constants derived from the mole fractions of four Tf species at 4 to 70% iron saturation were calculated as $K_{1C}:K_{1N}:K_{2C}:K_{2N} = 1: 0.86 \pm 0.1: 2.33 \pm 0.97: 2.03 \pm 1.02$ (*SI Appendix, Table S2*). The theoretical equilibrium distributions of the Tf species were generated from the equations in *SI Appendix,* Appendix S1 by using the relative equilibrium constants above and were represented as a continuous line (Fig. 4*B*). The excellent fit of the experimental and theoretical data suggests that the system reached equilibrium. Collectively, these results are consistent with the conclusion that equilibrium favors hinokitiol-mediated iron donation to both Tf binding sites to form monoferric Tf species. Furthermore, holo-Tf formed by additional iron atom transfer to either Fe$_C$Tf and Fe$_N$Tf has equivalent stability, as observed in the 1:1 ratio between K_{2N} and K_{2C}.
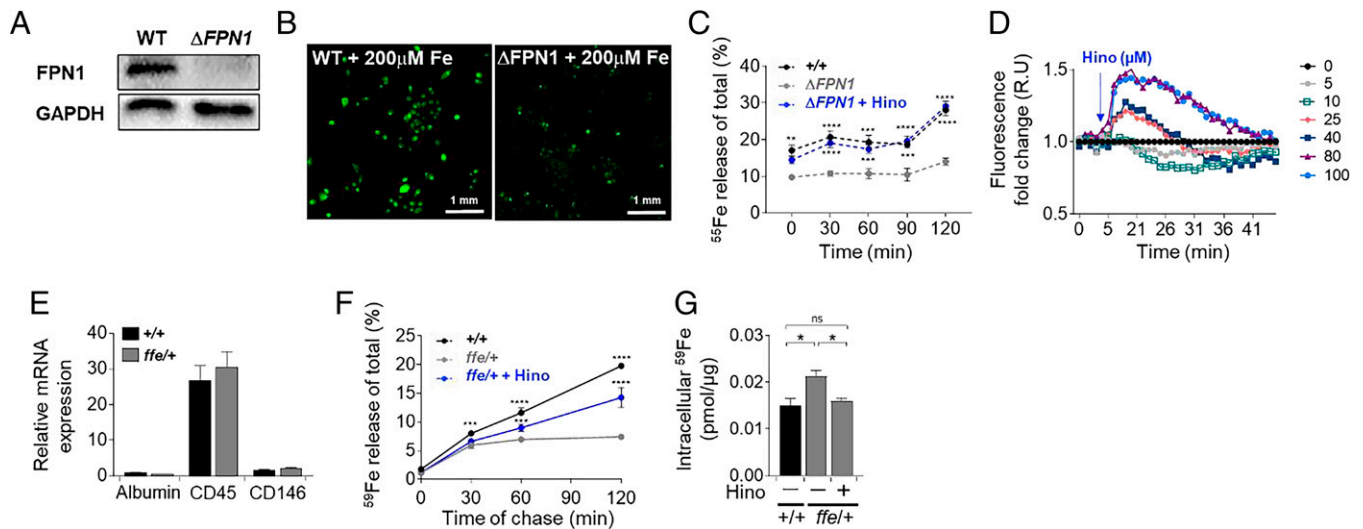
Fig. 3. Hinokitiol transports iron out of FPN1-deficient murine macrophages. (*A* and *B*) Molecular characterizations of FPN1-KO RAW264.7 cells. (*A*) Representative Western blot of FPN1 levels in the total cell lysates isolated from wildtype (WT) and $\Delta FPN1$ cells. (*B*) Representative images of FPN1-KO RAW264.7 cells treated with calcein. Intracellular labile iron detection in FPN1-KO RAW264.7 cells after iron loading. (Scale bar: 1 mm.) (*C* and *D*) Iron transport out of FPN1-KO RAW264.7 cells. (*C*) Radioactive iron assay revealed iron release upon treatment with 5 µM hinokitiol. Results are means ± SEM ($n = 8$ samples/group). Three independent experiments were performed yielding similar results. All data were compared with $\Delta FPN1$ at each time point. **$P < 0.01$, ***$P < 0.001$, and ****$P < 0.0001$ by two-way ANOVA with Tukey's multiple comparison test. (*D*) Representative calcein fluorescence measurement from three independent experiments performed in triplicate. Intracellular levels of labile iron were decreased in a concentration-dependent manner as measured using calcein. Fluorescence data were normalized to DMSO $t = 0$. (*E*) Mitochondrial RNA quantification of markers of hepatocytes (albumin), Kupffer cells (CD45), and endothelial cells (CD146) in isolated primary Kupffer cells. (*F* and *G*) Iron transport from primary Kupffer cells derived from *ffe/+* mice. Results are means ± SEM ($n = 4$ samples/group). Three independent experiments were performed yielding similar results. (*F*) Time course measurement of ^{59}Fe efflux into the extracellular media. Results are means ± SEM ($n = 3$ samples/group). Three independent experiments were performed yielding similar results. All data were compared with *ffe/+* at each time point. ***$P < 0.001$ and ****$P < 0.0001$ by two-way ANOVA with Tukey's multiple comparison test. (*G*) Measurement of intracellular ^{59}Fe levels after 60 min following treatment with 5 µM hinokitiol. Results are means ± SEM ($n = 3$ samples/group). Three independent experiments were performed yielding similar results. All data were compared with *ffe/+* at each time point. *$P < 0.05$ by one-way ANOVA with Tukey's multiple comparison test.

Ferrokinetic studies in adult male humans showed that serum iron trafficking to the bone marrow occurs within 10 min and peaks after 4 h, before falling rapidly by day 4 (40, 41). If the hemoglobinization observed in *ffe/+* mice occurred in a Tf-dependent manner, hinokitiol should transfer its bound iron to Tf faster than the serum iron clearance rate. We thus sought to study the kinetic properties of iron transfer from Fe(Hino)$_3$ to Tf (42–44). With excess apo-Tf, we measured the time-dependent absorbance of Fe(Hino)$_3$ at 420 nm using ultraviolet-visible spectroscopy. We then derived the pseudo first-order rate constants (k_{obs}) using the equations in *SI Appendix*, Appendix S2 (*SI Appendix*, Table S3). Curve fitting of these k_{obs} at various excess apo-Tf concentrations (Fig. 4*C*) revealed the second-order rate constant (k') and the rate constant at saturating apo-Tf concentration (k_{max}) (*SI Appendix*, Table S4). We used a 5:1 concentration of apo-Tf: Fe(Hino)$_3$ as our lowest ratio in order to maintain the condition of a pseudo first-order reaction (Fig. 4*C*). These data collectively suggest that iron transfer from hinokitiol to Tf occurs within 75 s. This rapid transfer of hinokitiol-bound iron to Tf is consistent with hinokitiol-mediated hemoglobinization occurring in a Tf-dependent pathway. Moreover, these in vitro results are in line with the increased Tf saturation observed in *ffe/+* mice following hinokitiol treatment (Fig. 2*E*).

We further asked whether the presence of free hinokitiol, which binds iron at high affinity (26), can interfere with Tf-dependent hemoglobinization. First, we conducted a competition assay between holo-Tf and various concentrations of hinokitiol. The holo-Tf level in the serum ranges between 4.38 and 19.79 µM (45, 46). Hinokitiol started to remove iron from 12.5 µM holo-Tf with a half-maximal inhibitory concentration (IC$_{50}$) of 165 µM (Fig. 4*D*). To determine circulating

levels of hinokitiol upon administration, we conducted pharmacokinetic studies using an IP injection of 30 mg/kg and 100 mg/kg hinokitiol to C57BL/6J mice (Fig. 4*E*). We found that 30 mg/kg was the lowest dose that allowed high-performance liquid chromatography detection of hinokitiol and accurate characterization of hinokitiol pharmacokinetics. The half-lives of hinokitiol were ~0.5 h (30 mg/kg) and 1 h (100 mg/kg), indicating rapid elimination from circulation. This rapid elimination was supported by the short mean residence time of hinokitiol. We also noted hinokitiol concentrations of ~150 µM and 500 µM in the plasma at 15 min after IP injection of 30 mg/kg and 100 mg/kg, respectively. Extrapolation from these data suggested that the use of a 10-mg/kg dose for chronic treatment of *ffe/+* mice could generate serum hinokitiol concentrations below 50 µM at 15 min postadministration. Collectively, these results suggest that hinokitiol will not remove iron from Tf at the doses administered in the in vivo experiments.

Next, we tested whether holo-Tf-dependent iron uptake into RBC progenitors could proceed in the presence of physiologically relevant concentrations of hinokitiol. We observed that free hinokitiol did not interfere with Fe$_2$Tf uptake into murine erythroleukemia (MEL) cells (Fig. 4*F*). Furthermore, to probe Tf-dependent hemoglobinization, we used anti-TfR1 R17 217 that has been reported to deplete cell surface TfR1 levels (47) in order to block holo-Tf internalization into the cells. This inhibition was evaluated by measuring ^{55}Fe$_2$Tf internalization into MEL cells (Fig. 5*B* and *SI Appendix*, Fig. S6 *A–D*). Consistent with Fig. 4*F*, free hinokitiol did not affect hemoglobinization in both IgG control and anti-TfR1 groups (Fig. 4*G*), suggesting that free hinokitiol does not interfere with Tf biology.

We further investigated the effect of hinokitiol-mediated iron transfer on hemoglobinization by differentiation of MEL
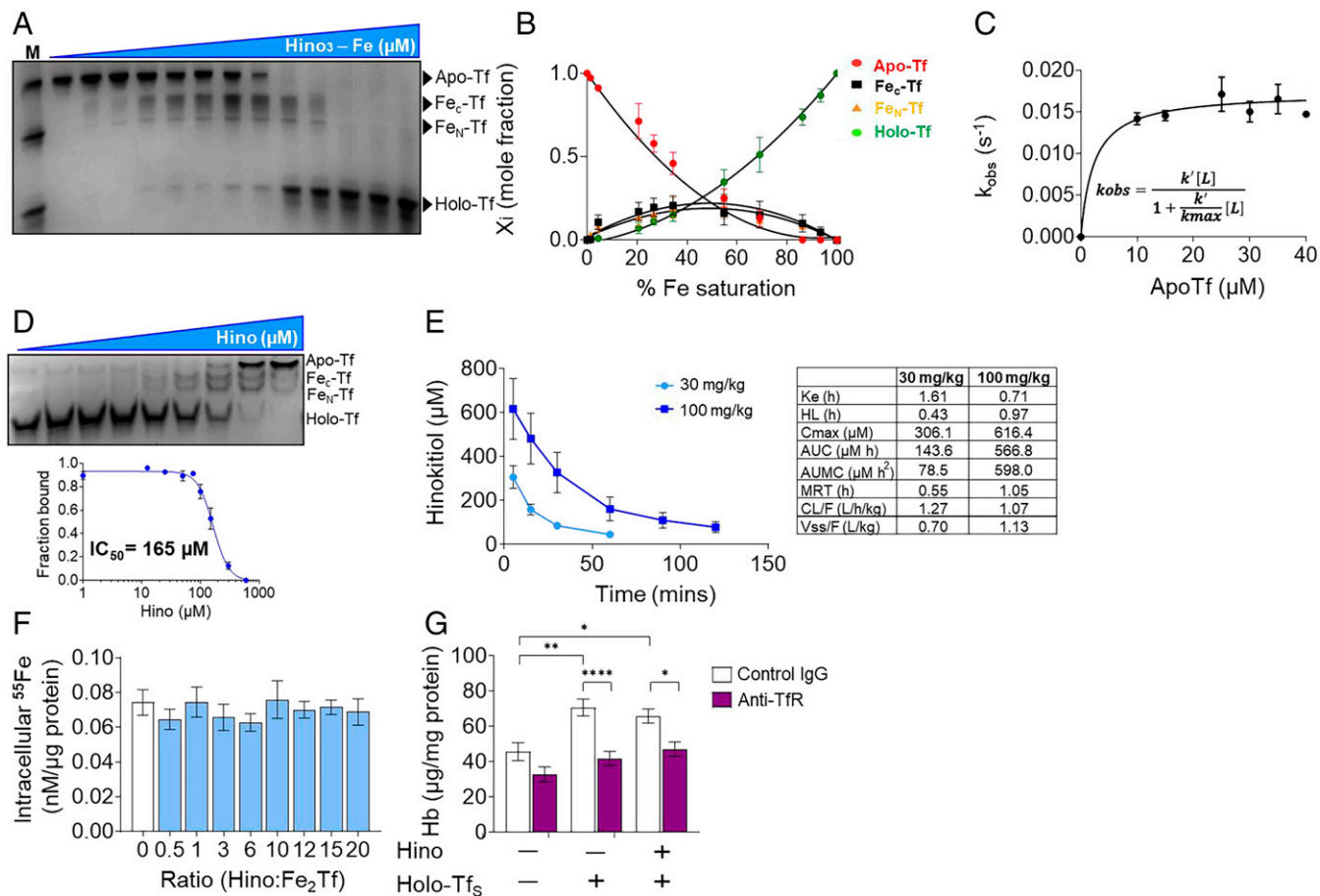
Fig. 4. Iron is transferred from hinokitiol to apotransferrin. (*A* and *B*) A total of 4 μM apo-Tf was incubated overnight with various concentrations of Fe(Hino)$_3$ to study the thermodynamics of iron transfer. [Apo-Tf]:[Fe-Hino] = 1: 0, 0.125, 0.25, 0.4, 0.5, 0.6, 0.8, 1, 1.25, 1.5, 2, 3, 4. (*A*) The first lane is a marker to denote various Tf species. Different Tf species were separated on a 10% tris-borate-ethylenediamine tetraacetic acid urea gel. (*B*) Mole fractions of the corresponding Tf-Fe complexes formed at each apo-Tf: Fe(Hino)$_3$ ratio were graphed according to *SI Appendix*, Appendix S1. Results are means ± SEM (*n* = 3 to 4 samples/group) from two independent experiments. (*C*) Pseudo first kinetic rate constants (k$_{obs}$) at various apo-Tf concentrations were graphed according to *SI Appendix*, Appendix S2. Results are means ± SEM from 5 to 6 independent experiments. (*D*) Titration of 12.5 μM holo-Tf with various concentrations of hinokitiol was measured using urea gel. Results are means ± SEM (*n* = 3 samples/group). Two independent experiments were performed yielding similar results. (*E*) Pharmacokinetics of hinokitiol in mice following IP injection of 30 mg/kg or 100 mg/kg hinokitiol and its pharmacokinetic parameters. Abbreviations: k$_e$, elimination rate constant; HL, half-life; C$_{max}$, maximum concentrations; AUC, area under the plasma concentration-time curve; AUMC, area under the first moment curve; MRT, mean residence time; CL/F, apparent clearance after extravascular administration; Vss/F, volume of distribution after extravascular administration. Results are means ± SEM (*n* = 3 samples/group). At least two independent experiments were performed yielding similar results. (*F*) Intracellular ^{55}Fe levels in MEL cells pulsed with 0.165 μM ^{55}Fe$_2$Tf and treated with various biologically-relevant ratios of [hinokitiol]:[Fe$_2$Tf]. Results are means ± SEM (*n* = 8 samples/group). Three independent experiments were performed yielding similar results. (*G*) Hemoglobin level measured in MEL cells differentiated with 5 μM holo-Tf$_S$ in the presence of 1 μM hinokitiol (+) behaved similarly to no-hinokitiol-treated (−) group. Results are means ± SEM (*n* = 3 samples/group) from at least three independent experiments performed in triplicate. *P < 0.05, **P < 0.01, and ****P < 0.0001 by two-way ANOVA with Tukey's multiple comparison test.

cells using holo-Tf preformed by mixing Fe(Hino)$_3$ and apo-Tf, designated as holo-Tf$_H$ (*SI Appendix*, Fig. S5*B*). Due to the multiple steps of purification, purified holo-Tf$_H$ lost some of its bound iron, resulting in a reduced holo-Tf level compared with holo-Tf$_S$. As a result, holo-Tf$_H$ yielded an ~25% reduced hemoglobin level in the IgG control group compared with the group treated with commercially available holo-Tf (holo-Tf$_S$) (Figs. 4*G* and 5*A*). Regardless, holo-Tf$_H$-mediated hemoglobinization was similarly reduced in the anti-TfR1 treatment group, suggesting that the phenomenon was dependent on the Tf/TfR1 pathway (Fig. 5*A*). Consistent with the results described above, the addition of free hinokitiol did not affect MEL differentiation mediated by holo-Tf. Overall, Fig. 5*A* highlights the last step in the mechanism of hinokitiol-induced hemoglobinization (Fig. 1*B*), in which the iron transfer from hinokitiol to apo-Tf (Fig. 4 *A* and *B*) to form holo-Tf$_H$ (*SI Appendix*, Fig. S5*B*) is used by the differentiating MEL cells to produce hemoglobin.

We then asked whether Fe(Hino)$_3$ could independently induce MEL differentiation into RBCs. We hypothesized that

since hinokitiol can mobilize iron across the membrane, Fe(Hino)$_3$-treated cells should have sufficient iron to overcome TfR1 inhibition for hemoglobin production. First, we probed whether hinokitiol could independently deliver iron to TfR1-inhibited MEL cells during MEL cell differentiation by measuring the internalization of ^{55}Fe exogenously delivered as a preformed ^{55}Fe(Hino)$_3$ complex. At day 0 to 1, ^{55}Fe(Hino)$_3$ caused some degree of internalization of ^{55}Fe, and similar intracellular iron levels were observed without and with TfR1 inhibition (Fig. 5*C*). Further studies showed that this capacity for Fe(Hino)$_3$ to independently mobilize iron into the cells was concentration dependent (*SI Appendix*, Fig. S6 *A* and *B*). However, the levels of internalization of ^{55}Fe remained relatively modest in these experiments (maxing out at 1 to 2 nM iron/μg protein). In contrast, under these same conditions of MEL cell differentiation, Tf-dependent iron uptake was faster and greater and continued to increase (*SI Appendix*, Fig. S6 *A* and *B*). At day 1 to 2 of MEL cells differentiation, the amount of ^{55}Fe that was internalized was 2 to 3 times greater when delivered in
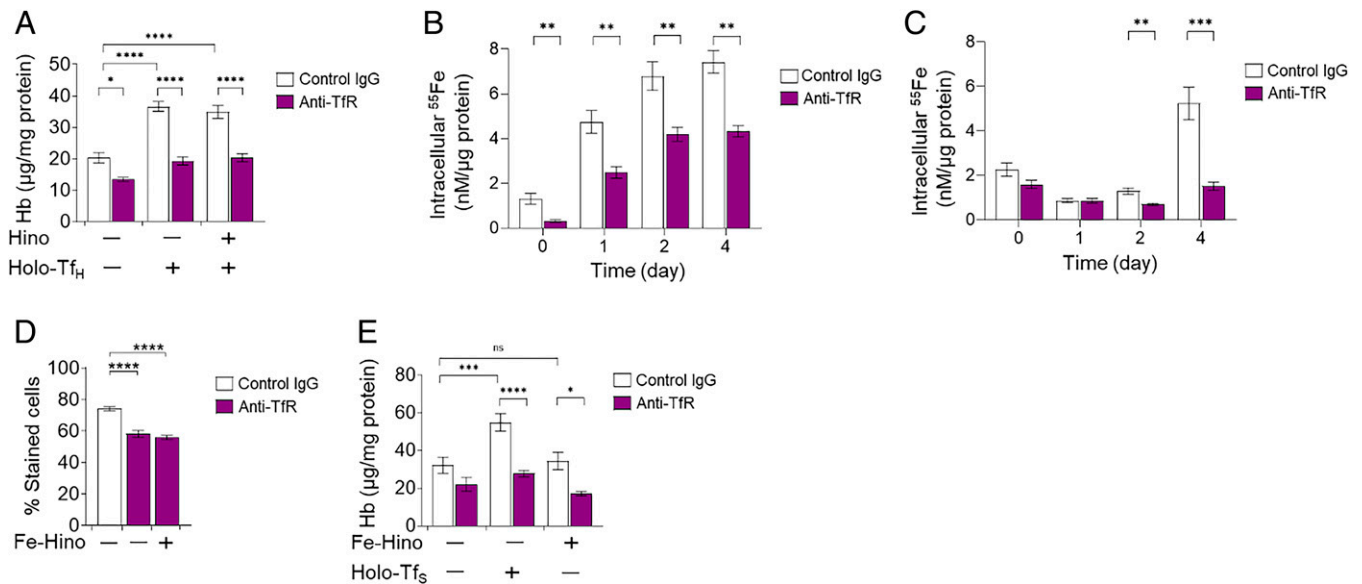
Fig. 5. Hinokitiol induces hemoglobinization via a Tf-dependent pathway. (*A*) Hemoglobin (Hb) measurement of MEL cells differentiated using 5 μM holo-Tf$_H$ with and without the presence of 1 μM hinokitiol (Hino). Results are means ± SEM ($n = 3$ samples/group) from three independent experiments. *$P < 0.05$ and ****$P < 0.0001$ by two-way ANOVA with Tukey's multiple comparison test. (*B* and *C*) Time course measurement of intracellular ^{55}Fe levels in differentiating MEL cells pulsed with 0.33 μM of precomplexed (*B*) ^{55}Fe$_2$Tf and (*C*) ^{55}Fe(Hino)$_3$. Day 0 denotes 30 min after ^{55}Fe pulsing. Results are means ± SEM ($n = 3$ samples/group) from three independent experiments. **$P < 0.01$ and ***$P < 0.001$ by multiple Student's t test with Bonferroni's correction. (*D*) Quantification of MEL cells stained with *o*-dianisidine relative to total cells. Cells were treated with and without 0.33 μM Fe(Hino)$_3$. Results are means ± SEM ($n = 3$ to 4 samples/group) from three independent experiments. ****$P < 0.0001$ by one-way ANOVA with Tukey's multiple comparison test. (*E*) Hb measurement of MEL cells differentiated using either 5 μM holo-Tf$_S$ or 0.33 μM Fe(Hino)$_3$ complex as the iron source. Results are mean ± SEM ($n = 3$ samples/group) from three independent experiments. *$P < 0.05$, ***$P < 0.001$, and ****$P < 0.0001$ by two-way ANOVA with Tukey's multiple comparisons test.

the form of ^{55}Fe$_2$Tf (Fig. 5 *B* and *C* and *SI Appendix,* Fig. S6 *B* and *C*). Of note, from day 2 onward, internalization of ^{55}Fe that was originally administered in the form of ^{55}Fe(Hino)$_3$ became sensitive to the inhibition of the TfR1 (Fig. 5*C* and *SI Appendix,* Fig. S6*C*), suggesting that the ^{55}Fe had largely been transferred from Hino to unsaturated Tf in the growth media and Tf-dependent cellular iron uptake was predominant. Moreover, when we administered the highest concentration of Fe(Hino)$_3$ possible without causing Hino-mediated toxicity to MEL cells (0.33 μM Fe, 1 μM Hino), differentiation of MEL cells (Fig. 5*D*) and hemoglobinization (Fig. 5*E* and *SI Appendix,* Fig. S6*E*) remained sensitive to TfR1 inhibition. These findings showed that differentiating reticulocytes require Fe$_2$Tf as iron source, thus further supporting the conclusion that the restoration of hemoglobinization by hinokitiol in *ffe*/+ mice is Tf/TfR1 dependent. Overall, these data collectively support a mechanism in which a direct hand-off between Fe(Hino)$_3$ and Tf precedes Fe$_2$Tf/TfR1-mediated hemoglobinization in *ffe*/+ mice (Fig. 1B).

Hinokitiol Reduces Labile Iron and Ferritin in Primary Macrophages Derived from Human Patients with FD. Next, we tested hinokitiol-mediated iron redistribution in a more clinically-relevant system. We isolated monocytes from three FD patients harboring a G80S, N174I, or A77D FPN1 mutation, which cause mild, medium, and severe FD, respectively (23, 48) (Fig. 6*A*). The isolated monocytes were differentiated into primary macrophages as previously described (49). In these macrophages, FD severity was correlated to the scale of cellular labile iron retention (Fig. 6*B*). In line with the murine macrophage data, we observed a dose-dependent reduction in intracellular labile iron in macrophages derived from all three patients following hinokitiol treatment (Fig. 6 *C–E*). Notably, the extent of intracellular iron reductions increased in parallel with the initial amount of iron retained, providing evidence

that the restoration of iron homeostasis by hinokitiol is driven by the gradients that build up due to the FPN1 deficiencies. In addition to labile iron retention, the primary macrophages also displayed enhanced levels of ferritin following hemoglobin supplementation (Fig. 6*F*). Hinokitiol treatment caused a ferritin reduction in primary macrophages (Fig. 6*G*), suggesting that hinokitiol also affects nonlabile iron and restores iron homeostasis in the FPN1-deficient system.

Discussion

We showed that hinokitiol could redistribute iron from the liver to erythrocytes and restore hemoglobinization in FPN1-deficient *ffe*/+ mice through a Tf-dependent mechanism. These observations suggest that hinokitiol, or an optimized derivative, has potential as a treatment for induced or genetic iron misdistribution disorders that share in common a deficiency of FPN1 function. Such a treatment might benefit individuals with certain genetic deficiencies and/or millions of people suffering from anemia of inflammation associated with various diseases (14, 15, 17–19).

One key finding of our study is the detailed characterization of the mechanism by which this small molecule redistributes iron in *Fpn1*-deficient *ffe*/+ mice. Hinokitiol at a relatively low dose (10 mg/kg) reduced iron stores from the liver, especially from Kupffer cells, to levels that nearly matched, but did not fall below, those of wildtype littermates. These data suggest the presence of an interface between the small molecule mobilizer and the biological mechanisms that drive iron homeostasis. In addition, we observed that despite the partial recovery of serum iron, *ffe*/+ mice displayed a full recovery of hemoglobin and hematocrit values, suggesting that even an imperfect recovery of iron mobilizing activity was sufficient to induce hemoglobinization. This phenomenon is consistent with the concept of robustness (50). Specifically, we posit that due to the inherent
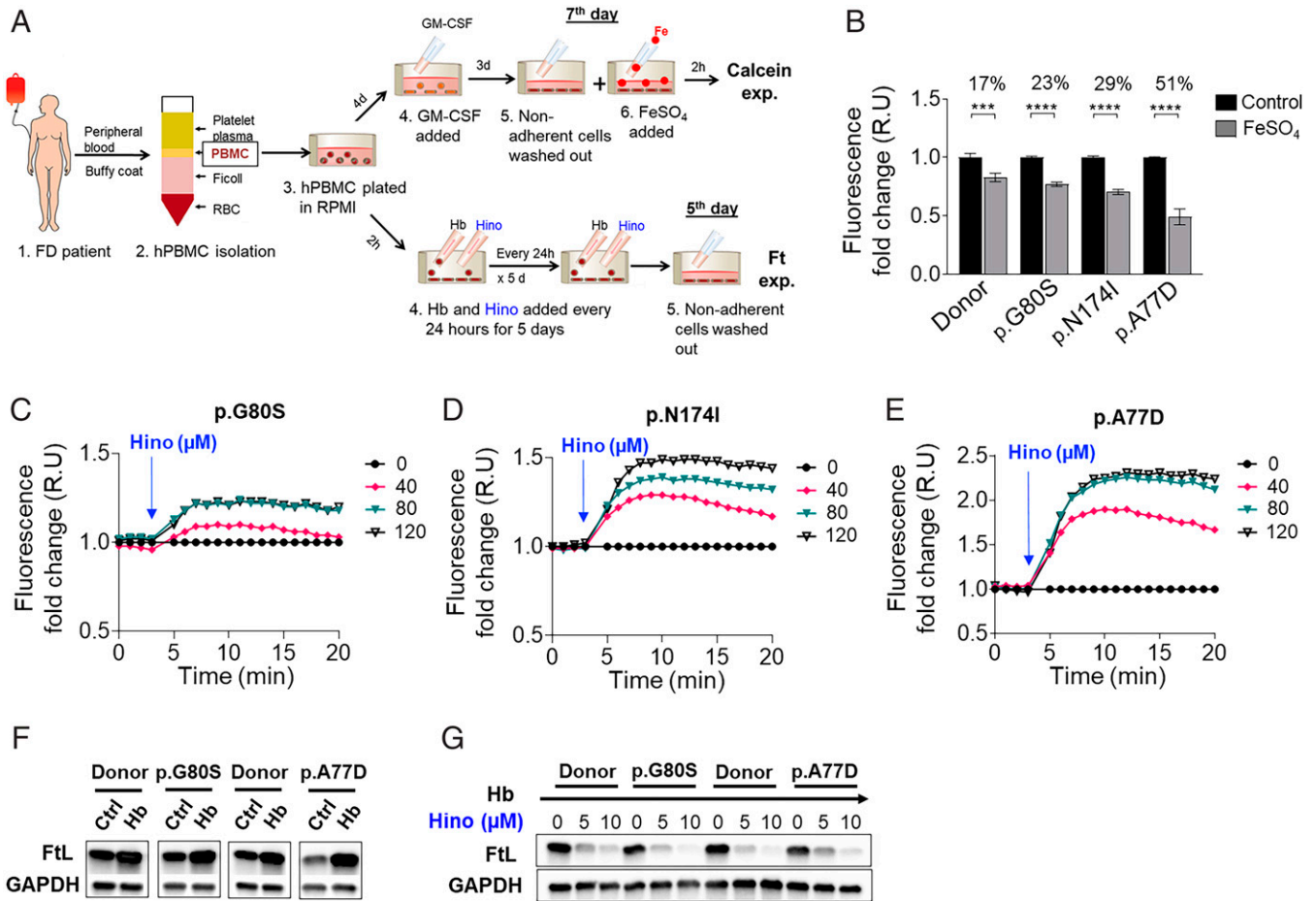
Fig. 6. Hinokitiol reduces levels of labile iron and ferritin (Ft) in primary macrophages derived from patients with FD. (*A*) Schematic representation of the experimental procedures for calcein and Ft experiments (*SI Appendix, SI Methods and Materials* for details). Abbreviations: GM-CSF, granulocyte-macrophage colony-stimulating factor; hPBMC, human peripheral blood mononuclear cells. (*B*) Retention of intracellular labile iron by primary macrophage cells from healthy donors or patients with FD harboring different mutations in FPN1 (pG80S, pN174I, or pA77D) was measured by changes in calcein fluorescence intensity upon addition of $FeSO_4$. Results are means ± SEM ($n = 3$ samples/group) from three independent experiments. ***$P < 0.001$ and ****$P < 0.0001$ by multiple Student's t test with Bonferroni's correction. R.U, relative units. (*C–E*) Representative calcein fluorescence measurement from three independent experiments performed in triplicate. Intracellular labile iron was decreased in $FeSO_4$-treated pG80S (*C*), pN174I (*D*), pA77D (*E*) macrophages after hinokitiol addition at the indicated concentration. The values are expressed as fold change over the reference cell value set to 1 (Ctrl [control] in *B*; FeSO4 in *C–E*). (*F* and *G*) A representative Western blot of three independent experiments performed in duplicate. Analysis of Ft expression in the whole-cell lysate of primary human macrophages obtained from healthy donors and patients with FD harboring pG80S or pA77D mutations following treatment with Hb (*F*) or Hb and hinokitiol (*G*) at the indicated concentrations.

robustness of hemoglobinization biology, even a small restoration of missing transmembrane iron transport function can drive the restoration of physiology.

FPN1 may also play a role in exporting iron out of erythrocytes to maintain systemic iron homeostasis and prevent RBCs from oxidative damage-mediated cell death (51). We thus note that hinokitiol-mediated transmembrane iron mobilization might also protect FPN1-deficient erythrocytes in *ffe*/+ mice from iron-induced oxidative damage. We cannot rule out the possibility that such an effect may contribute to the observed hinokitiol-mediated increases in hematocrit and hemoglobin levels in *ffe*/+ mice.

We demonstrated that a hand-off of iron atoms from hinokitiol to apo-Tf leads to stable formation of both monoferric and holo-Tf. Our kinetic studies further revealed that the iron transfer to apo-Tf was far faster than the reported time needed for Fe-Tf to reach the bone marrow. In all, both thermodynamic and kinetic studies support the hypothesis that the hemoglobinization relied on iron hand-off to Tf. In addition, hinokitiol-donated iron was shown to bind to both C- and N-terminal sites at the same level of affinity, both of which

could form holo-Tf with additional iron. As each monoferric Tf species has specific roles in iron homeostasis and erythropoiesis (52), this suggests that the hinokitiol-mediated formation of both Fe_CTf and Fe_NTf restores physiology without potentially disrupting the biological processes that utilize distinct monoferric Tf species.

Previously, we have shown that hinokitiol-mediated iron release from DMT1-deficient endosomes leads to hemoglobinization (26), suggesting that hinokitiol might be capable of restoring hemoglobinization in a Tf-independent manner. In order to probe this hypothesis, we used anti-TfR1 R17 217 to block the Tf/TfR1 pathway, which resulted in an ~50 to 60% reduction of hemoglobin levels in differentiated MEL cells. This variability in inhibition may be due to a difference in the cell viability used for the experiments since we have previously observed reduced hemoglobinization in the cells with viability lower than 90%. Iron uptake into differentiating MEL cells was shown to be substantially faster and more efficient when iron was delivered as Fe_2Tf vs. $Fe(Hino)_3$. We also observed that iron originally administered as $Fe(Hino)_3$ was eventually internalized into differentiating MEL cells in a manner that

was sensitive to TfR1 inhibition. These data are consistent with the conclusion that a direct hand-off between Fe(Hino)$_3$ and Tf in 10% fetal bovine serum-containing cell growth media (53) precedes Fe$_2$Tf/TfR1-mediated hemoglobinization and that the latter is an especially efficient mechanism for iron internalization to promote hemoglobinization. An experimentally-supported potential explanation for such efficiency is a direct interaction between Tf/TfR1 and mitochondria or to ferritin (kiss-and-run hypothesis) (54). Moreover, consistent with previous reports (55, 56), our data suggest that reticulocytes require Fe$_2$Tf as the iron source for differentiation into RBCs as these cells up-regulate TfR1 to fulfill their elevated iron needs (57). Furthermore, we showed that the highest concentration of Fe(Hino)$_3$ tolerable by MEL cells (0.33 µM Fe, 1 µM Hino) failed to overcome TfR1 inhibition to produce hemoglobin. This is another line of evidence that supports a hand-off of Fe from hinokitiol to Tf and that hemoglobinization is ultimately driven by the Tf/TfR1 pathway.

The lack of hinokitiol-mediated release of iron from the spleen may be due to a paucity of mobile iron in this tissue. Specifically, there is twofold more L-ferritin (per gram tissue) in the spleen than in the liver in wildtype mice (58). Based on this information, we hypothesize that more of the iron in splenic macrophages is ferritin bound/nonlabile and that this may explain why hinokitiol is less able to mobilize the iron retained in the spleen (26).

The *ffe*/+ mouse model recapitulates human FD, but it has certain limitations. We thus also tested hinokitiol's capacity in restoring iron homeostasis in primary macrophages derived from patients with FD. We found that in all of the patient-derived primary macrophages tested, hinokitiol caused the release of intracellular iron. Interestingly, hinokitiol treatment also caused a reduction in ferritin levels in these human macrophages. Although the mechanism by which hinokitiol reduces intracellular ferritin levels requires further studies, we hypothesize that ferritin was degraded as a cellular response to a hinokitiol-mediated decreased concentration of labile iron (59, 60).

Prior studies of small-molecule-mediated iron mobilization have previously been done with compounds salicylaldehyde isonicotinoyl hydrazone (SIH) and pyridoxal isonicotinoyl hydrazone (PIH) (61, 62). However, SIH and PIH failed to induce iron uptake and transport in a Caco-2 cell line deficient in DMT1 and FPN1, respectively (26), suggesting a distinct capacity for hinokitiol-mediated iron mobilization. Here, we show that a small molecule redistributes iron from sites of accumulation to sites of deficiency in vivo and that a small molecule can collaborate with iron-binding proteins to restore normal iron physiology.

The findings presented here provide a foundational platform for using hinokitiol or its variants to better understand the pathophysiology of the loss of function of iron transport proteins and the physiological consequences of iron redistribution. Our findings may also provide a foundation for the use of small molecule iron transporters as therapeutics for human diseases caused by iron misdistribution.

Materials and Methods

Materials. Hinokitiol was purchased from Sigma (catalog no. 469521). Fe(Hino)$_3$ was synthesized according to the protocol described previously (26), and the purity was verified by carbon/hydrogen/nitrogen analysis (*SI Appendix*, Table S5) and inductively coupled plasma mass spectrometry measurement of iron (*SI Appendix*, Table S6). Purified human apo-Tf (catalog no. T1147), holo-Tf (catalog no. T4132), and 3,3′,5,5′-tetramethylbenzidine (catalog no. 860336) were purchased from Sigma.

Statistical Analysis. All experiments were performed in triplicate unless otherwise noted specifically, and all results are presented as the means ± SD or means ± SEM. Student's t test with Bonferroni's correction was used for multiple two-group comparisons, one-way analysis of variance (ANOVA) with Tukey's correction for multiple comparisons was used to compare more than two groups with one independent variable, and two-way ANOVA with Tukey's correction for multiple comparisons was used to compare more than two groups with two independent variables. All statistical analyses were carried out using GraphPad Prism 9 software, and statistical significance is indicated as $*P < 0.05$, $**P < 0.01$, $***P < 0.001$, and $****P < 0.0001$. n.s. indicates no significant difference.

Data Availability. All study data are included in the article and/or *SI Appendix*.

Author affiliations: [a]Department of Biochemistry, University of Illinois at Urbana–Champaign, Urbana, IL 61801; [b]Department of Nutritional Sciences, University of Michigan School of Public Health, Ann Arbor, MI 48109; [c]Department of Medical and Surgical Sciences for Children and Adults, University of Modena and Reggio Emilia School of Medicine, 41121 Modena, Italy; [d]Department of Chemistry, University of Illinois at Urbana–Champaign, Urbana, IL 61801; [e]Department of Pharmaceutical Sciences, Northeastern University, Boston, MA 02115; [f]Gordon Center for Medical Imaging, Department of Radiology, Massachusetts General Hospital and Harvard Medical School, Boston, MA 02114; [g]Department of Human Genetics, University of Michigan Medical School, Ann Arbor, MI 48109; [h]Department of Biomedical & Nutritional Sciences, University of Massachusetts Lowell, Lowell, MA 01854; [i]Carle Illinois College of Medicine, Urbana, IL 61801; [j]Carl R. Woese Institute for Genomic Biology, Urbana, IL 61801; and [k]Beckman Institute for Advanced Science and Technology, Urbana, IL 61801

1. S. Abboud, D. J. Haile, A novel mammalian iron-regulated protein involved in intracellular iron metabolism. *J. Biol. Chem.* **275**, 19906–19912 (2000).
2. A. Donovan et al., The iron exporter ferroportin/Slc40a1 is essential for iron homeostasis. *Cell Metab.* **1**, 191–200 (2005).
3. A. T. McKie et al., A novel duodenal iron-regulated transporter, IREG1, implicated in the basolateral transfer of iron to the circulation. *Mol. Cell* **5**, 299–309 (2000).
4. E. Nemeth et al., Hepcidin regulates cellular iron efflux by binding to ferroportin and inducing its internalization. *Science* **306**, 2090–2093 (2004).
5. M. W. Hentze, M. U. Muckenthaler, B. Galy, C. Camaschella, Two to tango: Regulation of Mammalian iron metabolism. *Cell* **142**, 24–38 (2010).
6. G. Weiss, L. T. Goodnough, Anemia of chronic disease. *N. Engl. J. Med.* **352**, 1011–1023 (2005).
7. M. R. Bleackley, R. T. Macgillivray, Transition metal homeostasis: From yeast to human disease. *Biometals* **24**, 785–809 (2011).
8. P. Brissot, E. Bardou-Jacquet, A. M. Jouanolle, O. Loréal, Iron disorders of genetic origin: A changing world. *Trends Mol. Med.* **17**, 707–713 (2011).
9. G. J. Anderson, Ironing out disease: Inherited disorders of iron homeostasis. *IUBMB Life* **51**, 11–17 (2001).
10. S. Sheth, G. M. Brittenham, Genetic disorders affecting proteins of iron metabolism: Clinical implications. *Annu. Rev. Med.* **51**, 443–464 (2000).
11. A. Pietrangelo et al., Hereditary hemochromatosis in adults without pathogenic mutations in the hemochromatosis gene. *N. Engl. J. Med.* **341**, 725–732 (1999).
12. A. Pietrangelo, The ferroportin disease. *Blood Cells Mol. Dis.* **32**, 131–138 (2004).
13. K. E. Finberg et al., Mutations in TMPRSS6 cause iron-refractory iron deficiency anemia (IRIDA). *Nat. Genet.* **40**, 569–571 (2008).
14. T. Ganz, E. Nemeth, Iron balance and the role of hepcidin in chronic kidney disease. *Semin. Nephrol.* **36**, 87–93 (2016).
15. S.-N. J. Song et al., Comparative evaluation of the effects of treatment with tocilizumab and TNF-α inhibitors on serum hepcidin, anemia response and disease activity in rheumatoid arthritis patients. *Arthritis Res. Ther.* **15**, R141 (2013).
16. L. Mascitelli, F. Pezzetta, J. L. Sullivan, Iron, hepcidin, and increased atherosclerosis in systemic lupus erythematosus. *Int. J. Cardiol.* **131**, e20–e21 (2008).
17. L. Wang et al., The bone morphogenetic protein-hepcidin axis as a therapeutic target in inflammatory bowel disease. *Inflamm. Bowel Dis.* **18**, 112–119 (2012).
18. J. A. Simcox, D. A. McClain, Iron and diabetes risk. *Cell Metab.* **17**, 329–341 (2013).
19. S. Lakhal-Littleton et al., Cardiac ferroportin regulates cellular iron homeostasis and is important for cardiac function. *Proc. Natl. Acad. Sci. U.S.A.* **112**, 3164–3169 (2015).
20. H. F. Hazlett et al., Altered iron metabolism in cystic fibrosis macrophages: The impact of CFTR modulators and implications for Pseudomonas aeruginosa survival. *Sci. Rep.* **10**, 10935 (2020).
21. Y. Kong et al., Ferroportin downregulation promotes cell proliferation by modulating the Nrf2-miR-17-5p axis in multiple myeloma. *Cell Death Dis.* **10**, 624 (2019).
22. V. Bach, G. Schruckmayer, I. Sam, G. Kemmler, R. Stauder, Prevalence and possible causes of anemia in the elderly: A cross-sectional analysis of a large European university hospital cohort. *Clin. Interv. Aging* **9**, 1187–1196 (2014).

23. A. Pietrangelo, Ferroportin disease: Pathogenesis, diagnosis and treatment. *Haematologica* **102**, 1972–1984 (2017).

24. S. Unal, A. Piperno, F. Gumruk, Iron chelation with deferasirox in a patient with de-novo ferroportin mutation. *J. Trace Elem. Med. Biol.* **30**, 1–3 (2015).

25. P. C. Santos *et al.*, Non-HFE hemochromatosis. *Rev. Bras. Hematol. Hemoter.* **34**, 311–316 (2012).

26. A. S. Grillo *et al.*, Restored iron transport by a small molecule promotes absorption and hemoglobinization in animals. *Science* **356**, 608–616 (2017).

27. I. E. Zohn *et al.*, The flatiron mutation in mouse ferroportin acts as a dominant negative to cause ferroportin disease. *Blood* **109**, 4174–4180 (2007).

28. Y. A. Seo, J. A. Elkhader, M. Wessling-Resnick, Distribution of manganese and other biometals in flatiron mice. *Biometals* **29**, 147–155 (2016).

29. Y. A. Seo, M. Wessling-Resnick, Ferroportin deficiency impairs manganese metabolism in flatiron mice. *FASEB J.* **29**, 2726–2733 (2015).

30. E. E. Johnson, M. Wessling-Resnick, Flatiron mice and ferroportin disease. *Nutr. Rev.* **65**, 341–345 (2007).

31. B. M. Raabe, J. E. Artwohl, J. E. Purcell, J. Lovaglio, J. D. Fortman, Effects of weekly blood collection in C57BL/6 mice. *J. Am. Assoc. Lab. Anim. Sci.* **50**, 680–685 (2011).

32. A. Pietrangelo, The ferroportin disease. *Clin. Liver Dis. (Hoboken)* **3**, 98–100 (2014).

33. L. Lin *et al.*, Iron transferrin regulates hepcidin synthesis in primary hepatocyte culture through hemojuvelin and BMP2/4. *Blood* **110**, 2182–2189 (2007).

34. T. Ganz, Macrophages and systemic iron homeostasis. *J. Innate Immun.* **4**, 446–453 (2012).

35. W. Kelton *et al.*, Reprogramming MHC specificity by CRISPR-Cas9-assisted cassette exchange. *Sci. Rep.* **7**, 45775 (2017).

36. B. A. Napier, D. M. Monack, Creating a RAW264.7 CRISPR-Cas9 genome wide library. *Bio Protoc.* **7**, e2320 (2017).

37. C. I. Raje, S. Kumar, A. Harle, J. S. Nanda, M. Raje, The macrophage cell surface glyceraldehyde-3-phosphate dehydrogenase is a novel transferrin receptor. *J. Biol. Chem.* **282**, 3252–3261 (2007).

38. M. C.-M. Chung, Stucture and function of transferrin. *Biochem. Educ.* **12**, 146–154 (1984).

39. N. D. Chasteen, J. Williams, The influence of pH on the equilibrium distribution of iron between the metal-binding sites of human transferrin. *Biochem. J.* **193**, 717–727 (1981).

40. A. Ten Pas, D. M. Leahy, E. J. Van Slyck, Iron kinetics. I. Clinical considerations. II. Methodology. *Henry Ford Hosp. Med. J.* **13**, 317–329 (1965).

41. M. Pollycove, R. Mortimer, The quantitative determination of iron kinetics and hemoglobin synthesis in human subjects. *J. Clin. Invest.* **40**, 753–782 (1961).

42. W. R. Harris, Z. Wang, Y. Z. Hamada, Competition between transferrin and the serum ligands citrate and phosphate for the binding of aluminum. *Inorg. Chem.* **42**, 3262–3273 (2003).

43. A. H. Hissen, M. M. Moore, Site-specific rate constants for iron acquisition from transferrin by the Aspergillus fumigatus siderophores N',N'',N'''-triacetylfusarinine C and ferricrocin. *J. Biol. Inorganic Chem.* **10**, 211–220 (2005).

44. A. Stintzi, K. N. Raymond, Amonabactin-mediated iron acquisition from transferrin and lactoferrin by *Aeromonas hydrophila*: Direct measurement of individual microscopic rate constants. *J. Biol. Inorg. Chem.* **5**, 57–66 (2000).

45. C. Byrnes *et al.*, Iron dose-dependent differentiation and enucleation of human erythroblasts in serum-free medium. *J. Tissue Eng. Regen. Med.* **10**, E84–E89 (2016).

46. G. Hetet, I. Devaux, N. Soufir, B. Grandchamp, C. Beaumont, Molecular analyses of patients with hyperferritinemia and normal serum iron values reveal both L ferritin IRE and 3 new ferroportin (slc11A3) mutations. *Blood* **102**, 1904–1910 (2003).

47. J. F. Lesley, R. J. Schulte, Inhibition of cell growth by monoclonal anti-transferrin receptor antibodies. *Mol. Cell. Biol.* **5**, 1814–1821 (1985).

48. I. De Domenico *et al.*, Molecular and clinical correlates in iron overload associated with mutations in ferroportin. *Haematologica* **91**, 1092–1095 (2006).

49. G. Montosi *et al.*, Wild-type HFE protein normalizes transferrin iron accumulation in macrophages from subjects with hereditary hemochromatosis. *Blood* **96**, 1125–1129 (2000).

50. J. A. de Visser *et al.*, Perspective: Evolution and detection of genetic robustness. *Evolution* **57**, 1959–1972 (2003).

51. D.-L. Zhang, M. C. Ghosh, H. Ollivierre, Y. Li, T. A. Rouault, Ferroportin deficiency in erythroid cells causes serum iron deficiency and promotes hemolysis due to oxidative stress. *Blood* **132**, 2078–2087 (2018).

52. N. L. Parrow *et al.*, Lobe specificity of iron binding to transferrin modulates murine erythropoiesis and iron homeostasis. *Blood* **134**, 1373–1384 (2019).

53. K. Kakuta, K. Orino, S. Yamamoto, K. Watanabe, High levels of ferritin and its iron in fetal bovine serum. *Comp. Biochem. Physiol. A Physiol.* **118**, 165–169 (1997).

54. P. Ponka, Tissue-specific regulation of iron metabolism and heme synthesis: Distinct control mechanisms in erythroid cells. *Blood* **89**, 1–25 (1997).

55. R. J. Walsh, E. D. Thomas, S. K. Chow, R. G. Fluharty, C. A. Finch, Iron metabolism. Heme synthesis in vitro by immature erythrocytes. *Science* **110**, 396–398 (1949).

56. D. W. Allen, J. H. Jandl, Kinetics of intracellular iron in rabbit reticulocytes. *Blood* **15**, 71–81 (1960).

57. E. F. Gautier *et al.*, Comprehensive proteomic analysis of human erythropoiesis. *Cell Rep.* **16**, 1470–1484 (2016).

58. C. Ferreira *et al.*, H ferritin knockout mice: A model of hyperferritinemia in the absence of iron overload. *Blood* **98**, 525–532 (2001).

59. V. Picard, S. Epsztejn, P. Santambrogio, Z. I. Cabantchik, C. Beaumont, Role of ferritin in the control of the labile iron pool in murine erythroleukemia cells. *J. Biol. Chem.* **273**, 15382–15386 (1998).

60. A. M. Konijn *et al.*, The cellular labile iron pool and intracellular ferritin in K562 cells. *Blood* **94**, 2128–2134 (1999).

61. P. Ponka, D. Richardson, E. Baker, H. M. Schulman, J. T. Edward, Effect of pyridoxal isonicotinoyl hydrazone and other hydrazones on iron release from macrophages, reticulocytes and hepatocytes. *Biochim. Biophys. Acta* **967**, 122–129 (1988).

62. P. Ponka, J. Borová, J. Neuwirt, O. Fuchs, Mobilization of iron from reticulocytes. Identification of pyridoxal isonicotinoyl hydrazone as a new iron chelating agent. *FEBS Lett.* **97**, 317–321 (1979).